ELSEVIER

Journal of Alloys and Compounds 426 (2006) 357–362

Journal of
ALLOYS
AND COMPOUNDS

www.elsevier.com/locate/jallcom

Formation of one-dimensional MgH_2 nano-structures by hydrogen induced disproportionation

Claudia Zlotea [a,*], Jun Lu [b], Yvonne Andersson [a]

[a] Department of Materials Chemistry, Uppsala University, Box 538, Uppsala 751 21, Sweden
[b] Microstructure Laboratory, Uppsala University, Box 534, Uppsala 751 21, Sweden

Received 25 January 2006; received in revised form 16 February 2006; accepted 16 February 2006

Abstract

Remarkable formation of one-dimensional single crystalline MgH_2 structures in the nano- and micro-meters ranges is reported. These structures have been tailored by hydrogen absorption and subsequent disproportionation of bulk $Mg_{24}Y_5$. The MgH_2 whiskers have been structurally and morphologically characterized by X-rays diffraction, scanning and transmission electron microcopies. A growth model is proposed for the early stage of the whiskers formation by combining surface chemical and morphological investigations. The formation of MgH_2 whiskers opens new engineering explorations and challenges for further experimental and theoretical studies.

Keywords: Magnesium hydride; One-dimensional nano-structures; Hydrogen absorbing materials

1. Introduction

The shape, size, surface composition and crystal structure of materials are major factors that control the hydrogen absorption properties for energy storage applications. To act as an efficient energy carrier, hydrogen should be absorbed and desorbed in materials easily and in high quantities. Magnesium is one of the most promising candidates for future hydrogen storage materials due to the formation of MgH_2, where the hydrogen content corresponds to 7.6 wt.%. However, pure Mg presents major drawbacks for use in robust, sustainable and long life storage device. The Mg hydride formation is very slow and has poor thermodynamic properties [1,2]. In order to overcome these drawbacks, two promising ways have been extensively investigated. One route is to reduce the Mg particle size to micro- or nano-ranges and the other solution is to tailor Mg-rich alloys and compounds. Several studies have been reported on nano-structured Mg materials by mechanical synthesis [3]. This approach addresses the kinetic problem of hydrogen diffusion. The uptake tends to stop once the hydride layer formed at the surface exceeds 30–50 μm and is considered to originate from the very slow hydrogen diffusion through the β-MgH_2 layer [2]. Alloying Mg is a possible solution to overcome the inherent limitations of pure Mg [1,4]. For example, the kinetics of the hydrogen absorption in Mg_2Ni is found to be significantly faster than in pure Mg [5]. Mg_2Ni absorbs hydrogen but the uptake capacity is decreased as compared to Mg [6]. So far, no valid solution for hydrogen storage material for sustainable devices has been proposed. To alloy Mg with Y might be a plausible route, since our recent study on $Mg_{1-x}Y_x$ ($x=0$–0.17) thin films has demonstrated that the presence of yttrium improves the diffusion of hydrogen [7]. The present study reports on the possibility of tailoring new one-dimensional Mg-based structures in the nano- and micro-meters ranges by hydrogen absorption and disproportionation of bulk $Mg_{24}Y_5$. The formation of MgH_2 whiskers by hydrogen absorption and subsequent disproportionation of bulk alloys has never been reported so far. The proposed method has the unique advantage of designing nano- and micro-structures directly from the bulk material without contamination introduced by mechanical alloying synthesis techniques. Comparable formation of metallic Mg whiskers has been reported earlier [8].

2. Experimental methods

$Mg_{24}Y_5$ bulk compounds were prepared from appropriate amount of the elements: Y 99.9% purity (Highways International) and Mg 99.95% purity (Alfa

---

* Corresponding author. Present address: European Commission, Directorate-General, Joint Research Center, Institute for Energy, P.O. Box 2, NL-1755 ZG Petten, The Netherlands.

E-mail address: claudia.zlotea@gmail.com (C. Zlotea).

0925-8388/$ – see front matter © 2006 Elsevier B.V. All rights reserved.
doi:10.1016/j.jallcom.2006.02.024

Aesar). The elements were placed in a Ta tube, which is sealed by welding in an Ar atmosphere and subsequently heated up to 1073 K in a high frequency induction furnace under 300 mbar of Ar. In order to avoid long time air exposure, the samples were manipulated and stored inside a glove box under Ar atmosphere. Prior to any characterization, the powder samples were ground and filtered to particle sizes less then 60 μm.

Hydrogen absorptions were performed through the gas–solid interaction using an autoclave system at different hydrogen pressures and temperature profiles. Prior to hydrogen absorption, the system was evacuated to a base pressure of 10^{-2} mbar and flushed several times with hydrogen gas. The hydrides were prepared by repeating several heat-treatments in hydrogen atmosphere in order to crack the oxide layer and to ensure a direct access of hydrogen to the pure compound. The temperature profile was 1 h heating to 643 K, 5–20 h dwelling and 8 h cooling to 300 K, 2–5 times at the applied hydrogen pressure.

The structural properties were determined by X-rays diffraction (XRD) measurements using a Guinier-Hägg camera with Cu Kα1 radiation and Si as internal standard. The experimental crystallographic constants were refined using the CELREF program based on the least-squares method. $Mg_{24}Y_5$ crystallizes in the cubic α-Mn type structure with the refined lattice parameter $a = 11.257(2)$ Å, which is in good agreement with earlier results [9–11]. In the XRD pattern of $Mg_{24}Y_5$, extra diffraction peaks with very weak intensities were observed and were identified as Mg_2Y.

Surface analyses of the initial compound were performed at room temperature by X-rays photoelectron spectroscopy (XPS) measurements using a Phi Quantum 2000 instrument with a monochromatic Al Kα source (1486.6 eV). In order to determine the surface and bulk chemical modulation with depth, selected areas were bombarded by Ar^+ and sequentially analyzed. The total sputtering time for depth profiling was approximately 7 min. The investigated electronic levels were Mg 2p, Y 3d and O 1s. Both metallic and oxidized Mg and Y atoms are present at the surface. The oxidized Mg and Y peaks completely vanish after approximately 1 min of sputtering. The binding energy of Mg 2p peak (49.8 eV) after 1 min of sputtering is in agreement with the value of pure Mg or other Mg-rich alloys [1]. The binding energy of the metallic Y 3d5/2 peak (156.4 eV) is shifted compared to the value of pure Y (155.8 eV) [12]. The chemical shift is understood in terms of changes in the atomic environment of Y occurring upon the compound formation. A surface segregation with Mg enrichment is evidenced since the Mg/Y ratio is approximately twice as large in the oxidized layer of the surface (after 40 s of Ar^+ sputtering) compared to the bulk (after 7 min of Ar^+ sputtering), which is in agreement with earlier studies [13]. Previously, it was established that the driving force towards surface segregation is the difference in surface energy of the alloying elements in vacuum conditions [14,15]. Within this model, Mg atoms will preferentially segregate to the surface, even before air contact.

Microstructural analyses were performed by scanning electron microscopy (SEM), energy dispersive spectroscopy (EDS) and transmission electron microscopy (TEM) techniques before and after heat-treatments in hydrogen atmosphere. The SEM measurements were carried out using a high resolution LEO 1550 microscope equipped with an in-lens detector. The TEM specimen was characterized by a Jeol2000FXII microscope operating at 200 kV. The EDS analysis was performed by an INCA instrument. The preparations of the specimens for SEM and TEM investigations were made by dispersing the powder materials on a carbon tape and a copper grid with a thin carbon film, respectively. Prior to the SEM and EDS measurements, the specimens were exposed to air.

3. Results and discussion

$Mg_{24}Y_5$, with a small homogeneity range on the Mg-rich side, crystallizes in a related cubic α-Mn type structure, space group I-43m [9–11]. According to the XPS measurements, the surface of the initial sample is enriched with Mg and partially covered with both Mg and Y oxides. The $Mg_{24}Y_5$ sample was exposed to different hydrogen pressures in the temperature range 550–650 K. $Mg_{24}Y_5$ starts to react with hydrogen at 573 K, but to crack the oxide layer and to ensure a direct access of hydrogen to the pure compound, the temperature has to be increased from 300 to 643 K several times. This heat-treatment in hydrogen atmosphere causes disproportionations of the compound for pressures between 1.5 and 30 bar. The obtained phases at different pressures, as determined by XRD, are shown in Table 1 and Fig. 1.

Table 1
Phases formed by hydrogen disproportionation of $Mg_{24}Y_5$ at different applied pressures (bar) at 643 K

$P(H_2)$ (bar)	Disproportionation phases
1.5–5	$YH_2 + Mg$
10	$YH_2 + Mg + MgH_2 + YH_3$
20–30	$YH_3 + MgH_2$

The results are obtained for 3 heat-treatment cycles in hydrogen atmosphere with a temperature profile of 1 h heating, 5–20 h dwelling and 8 h cooling to 300 K.

At hydrogen pressures below 5 bar, $Mg_{24}Y_5$ undergoes a complete disproportionation with the formation of YH_2 and metallic Mg. At hydrogen pressures above 10 bar, $Mg_{24}Y_5$ decomposes into YH_2, YH_3, MgH_2 and metallic Mg. The reaction rate was slow and thermodynamic equilibrium conditions were not obtained despite several heat-treatment cycles. At the hydrogen pressure of 20 bar, a complete reaction of Mg and Y with hydrogen occurs. Thermodynamic equilibrium is reached and only YH_3 and MgH_2 are seen in the XRD patterns. Y hydride might have a catalytic effect in the formation of MgH_2, as previously suggested for rare-earth hydrides in the Ce–Mg–H [16] and La–Mg–H [17] systems. Although, the role of the Y hydride in the formation of MgH_2 remains an open question and is still to address. The diffraction peaks of the Y hydrides are very broad indicating either small particles sizes or strain in the crystallites. These results allow us to propose a two-step mechanism for the hydrogen absorption of $Mg_{24}Y_5$. During the first step, YH_2 and pure metallic Mg are formed. The second step promotes the formation of YH_3 and MgH_2. The disproportionation mechanism can be understood in terms of the thermodynamics of elementary hydride formation. The heats of formation ΔH_f of YH_2, YH_3 and MgH_2 are −114, −89 and −37 kJ/mol H, respectively [18]. The formation of YH_2 is the most favorable, which explains

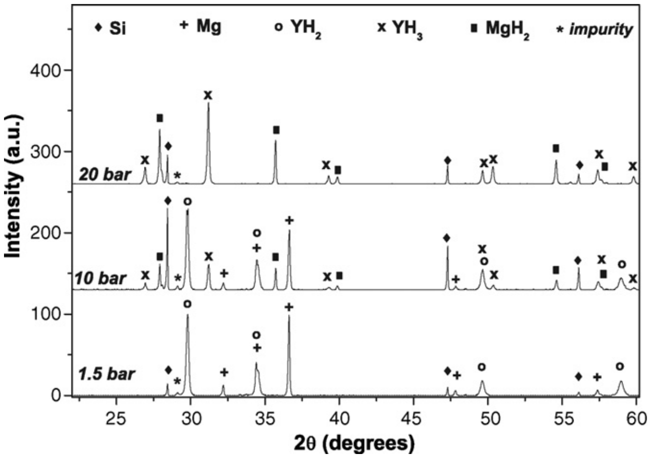

Fig. 1. XRD patterns of hydrogenated $Mg_{24}Y_5$ at 643 K and 1.5, 10 and 20 bar hydrogen pressures.

the presence of YH_2 already at moderate pressure. At higher pressures both MgH_2 and YH_3 are always formed, which is in agreement with the heats of formation.

Y is chemically related to the rare-earth metals and it is of interest to compare our results to previous studies of hydrogenation of rare-earth Mg alloys and compounds, with similar hydrogen disproportionation reactions [4,16,19]. RMg_{12}, R_2Mg_{17} and R_5Mg_{41} (R = La, Ce and mischmetal) form RH_3 and MgH_2 at hydrogen pressures between 5 and 50 bar in the temperature range 600–653 K [4]. An in situ X-rays diffraction study of $LaMg_{12}$ and La_2Mg_{17} has clearly shown direct decompositions into LaH_3 and MgH_2 at 10, 30 and 50 bar for the temperature range 553–603 K [19]. On the contrary, a calorimetric study demonstrates a two-step mechanism for hydrogen interactions in the La–Mg system [20], which is similar to our proposed model.

Microstructural studies have been performed by high resolution scanning electron microscopy (SEM) and energy dispersive spectroscopy (EDS) before and after hydrogen absorption at different pressures. The initial powder with particle sizes less than 60 μm showed a common particle morphology and size distribution. The SEM investigation performed after the first step of the hydrogen induced disproportionation demonstrated no significant changes in the morphology of the particles. A more compact particle size distribution was noticed and might be understood in terms of agglomeration due to the heat-treatments. However, a large number of cracks on the surface of the particles were formed after the first step of disproportionation. A nest-like microstructure with particles in the range of hundreds of nanometers can be seen between the cracks. This might be attributed to the disproportionation and formation of YH_2 and pure Mg.

Significant morphology changes were proved to be induced by the second step of the hydrogen induced disproportionation. Remarkable microstructures are shown in Fig. 2. A large number of one-dimensional structures with thicknesses in the range of nanometers (further called nano-whiskers), occasionally up to micrometers, were observed on the surface of the host particles of the parent compound.

The crystal symmetry and the approximate lattice parameters of the nano-whiskers were obtained from transmission electron microscopy measurements by selected area electron diffraction (SAED) (see Fig. 3). SAED patterns from two whiskers were acquired, which are illustrated in the insets of the Fig. 3.

The nano-whiskers are single crystals with tetragonal symmetry and the lattice parameters $a = b = 4.55(5)$ Å and $c = 3.00(5)$ Å. This result is consistent with the crystal structure of MgH_2, which crystallizes in space group *P42/mnm* with the general reflection conditions $0\,k\,l$: $k + l = 2n$, $0\,0\,l$: $l = 2n$ and $h\,0\,0$: $h = 2n$ [21]. It should be noted that the extinct reflection $\{1\,0\,0\}$ is weakly present in one of the SAED pattern. The thickness and width of the nano-whisker is about 120 nm, which is too thick for the kinematical condition to be valid and thus extinction reflections are present. No conclusion could be made regarding the crystallographic growth direction of the nano-whiskers. The identification of the nano-whiskers as MgH_2 was also supported by the EDS analysis, which showed that Mg is the main constituent element. Small amount of oxygen was detected in contrast with hydrogen, which cannot be observed by this method. A quantitative result cannot be proposed because of the smaller size of the nano-whiskers as compared to the interaction volume of the electron beam with the probed material.

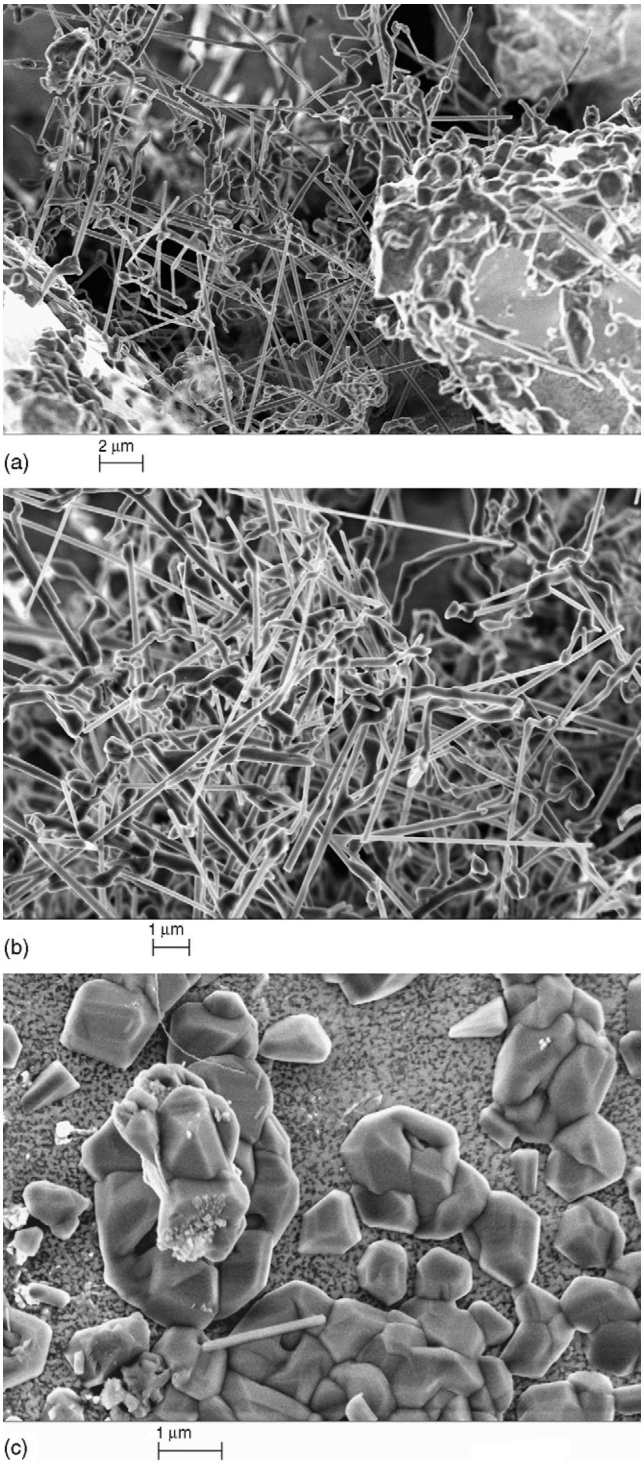

Fig. 2. SEM images obtained after the hydrogen induced disproportionation of bulk $Mg_{24}Y_5$ at 20 bar and 643 K: one-dimensional nano-structures grown on the host particles of the parent compound (a), net of one-dimensional nano-structures (b) and polyhedral grains on the surface of the host material (c).

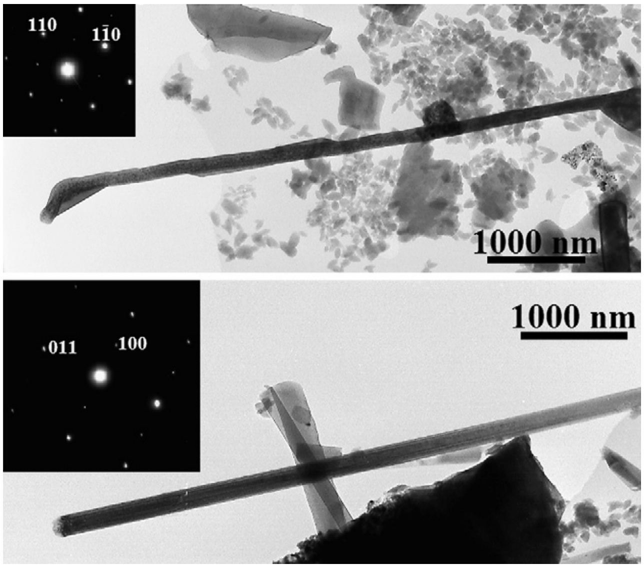

Fig. 3. TEM images of nano-whiskers obtained after hydrogen induced disproportionation of $Mg_{24}Y_5$ at 20 bar hydrogen pressure and 643 K. The insets show the selected area electron diffraction patterns.

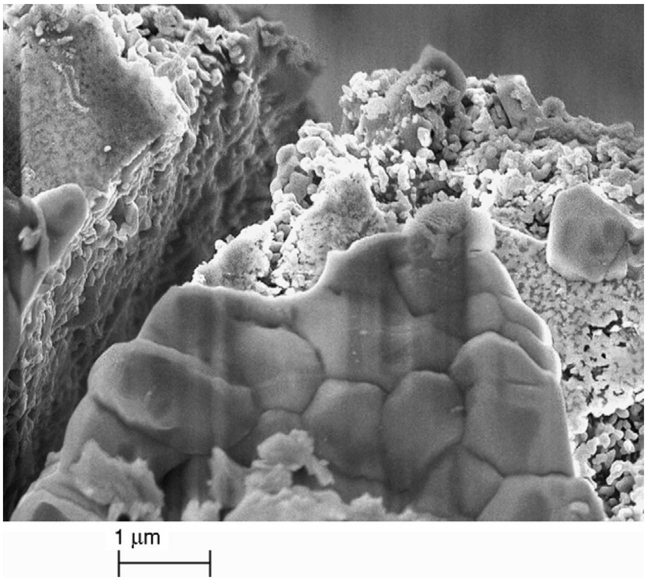

Fig. 4. SEM image of the surface of the host particle showing a microstructure of small grains (bright color) with thickness in the nanometer range. The agglomerates of polyhedral grains (dark color) correspond to the MgH_2 phase.

The MgH_2 nano-whiskers form complex three-dimensional nets interconnecting the particles of the initial compound (see Fig. 2a and b). A large number of nano-whiskers have straight and uniform widths along the growth direction. Kinked whiskers with complex shapes growing in irregular branches were also observed. Moreover, the nano-whiskers were interacting and deforming each other during the growth. The most extraordinary feature of these one-dimensional MgH_2 structures is the length, which occasionally exceeds 150 μm. As a general tendency, the density and numbers of nano-whiskers are increasing with the applied hydrogen pressure. They are very brittle and a great number is broken during the SEM or TEM specimen preparations and measurements.

Together with these unexpected one-dimensional structures, agglomerates of micro-particles were observed along cracks and on the surface of the particles (see Fig. 2c). These micro-particles have polyhedral regular shapes and sizes in the nano and micrometer ranges. A large number of MgH_2 nano-whiskers are originating from the polyhedral particles. One micro-particle can grow several nano-whiskers with different thicknesses and directions. We conclude that the polyhedral micro-particles are MgH_2 with different morphologies. This is also supported by EDS analysis, which revealed a Mg-rich composition and a small oxygen content (less then 3 at.%).

The microstructure of the parent particles revealed also interesting features. The surface of the particles contains a large number of cracks and flakes of the material. The fine structure of the parent particles was found to be very porous and formed by a large number of nano-particles (see Fig. 4). The average chemical composition of the porous particles, as determined by EDS, revealed a richer Y concentration as compared to the starting material. This result can be understood by long-range diffusion of Mg atoms towards the surface and formation of different MgH_2 morphologies.

The formation of nano-whiskers is most favorable after at least 3 heat-treatment cycles in hydrogen atmosphere at 643 K and pressures above 10 bar. Samples exposed to hydrogen pressure of 12 bar for 1 or 2 heat-treatment cycles in hydrogen atmosphere show a complete decomposition of the initial compound into YH_2, metallic Mg and small traces of both YH_3 and MgH_2. SEM investigations of these samples demonstrate that the early stage of the one-dimensional MgH_2 growth consists of very few whiskers without any polyhedral micro-particles. The microstructure revealed that several whiskers were growing compactly and the thickness of the single structures was between 100 and 200 nm (see Fig. 5a). The first whiskers extrude from the host particle in straight or kinked shapes by bursting the surface layer (see Fig. 5b). Further heat-treatment cycles in hydrogen atmosphere favor the formation of MgH_2 in both complex nets of nano-whisker and polyhedral micro-particles.

Several questions about the origin and growth mechanism of the MgH_2 nano-whiskers have been aroused. Several types of mechanism are currently accepted to well explain the growth of one-dimensional nano-structures [22–26]. The vapor–liquid–solid (VLS) process is the most used mechanism to understand the growth of semiconductor nano-whiskers [26]. A catalyst metal seed, which is located at the end of the whisker, always assists this process and its size influences the diameter of the whisker. Within this model, metallic Mg whiskers have been reported to grow from hydrogenated Mg powder [8]. The formation of Mg whiskers was assured by the presence of sublimed Mg vapor and hydrogen as carrier gas. Catalyst Mg-Al eutectic seeds were located at the tips of the whiskers. However, in our case, SEM or TEM investigations cannot detect any metal seeds at the ends of the MgH_2 whiskers. The vapor–solid (VS) process is widely used to describe the growth of nano-belts and nano-rods of oxides [23,24]. Within the VS mechanism, the oxide vapor directly deposits on a substrate at lower temperatures and

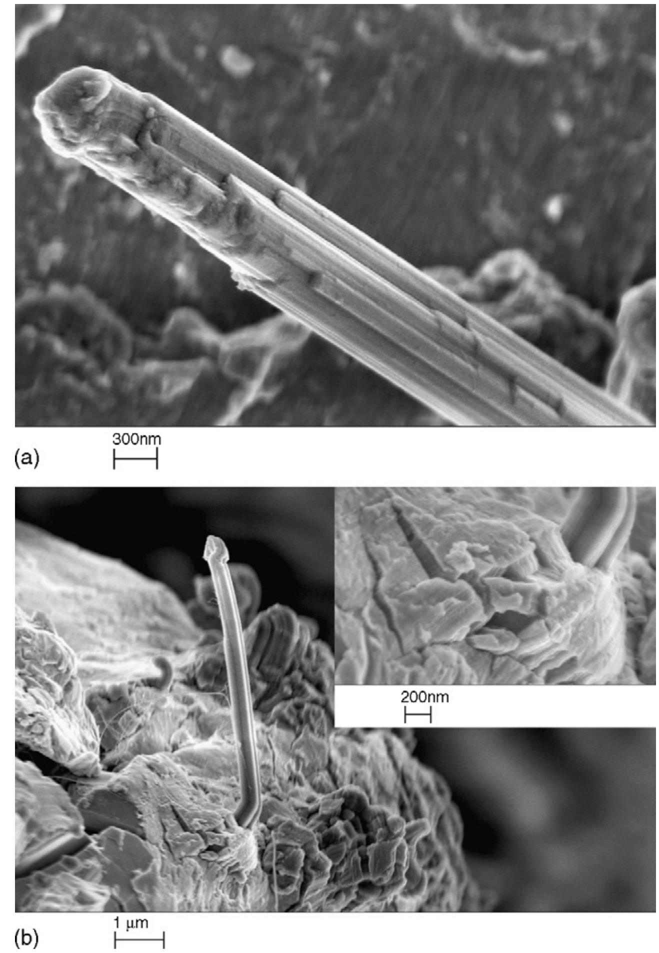

Fig. 5. SEM images of the early stage of nano-whiskers growth induced by hydrogen disproportionation of bulk $Mg_{24}Y_5$ at 12 bar, 643 K and 1–2 heat-treatment cycles in hydrogen atmosphere. A compact structure of several nano-whiskers with thickness between 100 and 200 nm can be observed (a). A whisker extrusion and the zoom of the cracked surface around the whisker base (b).

grows into different morphologies. MgO has been reported to grow into nano-rods or nano-belts structures by heating a halide source in a flow of argon–oxygen gas mixture [24,25]. The VLS and VS growth models are based on the fact that the reactants are supplied in the vapor phase. In our case, the growth process of the MgH_2 whiskers is far from clear. Either a vapor phase is formed during the hydrogen absorption or a long-range solid diffusion mechanism has to be taken into account. The starting hypothesis of gaseous reactants is believed to be hardly fulfilled in our hydrogenation conditions. The working temperature is 643 K and well below the melting point of metallic Mg (923 K). No evidence for loss of material or evaporation on the walls of the crucibles and autoclave were noticed, regardless the temperatures and pressures. Therefore, the VLS and VS models whiskers growth seem to be unlikely.

Many models are currently proposed in order to explain the spontaneous growth of the low melting point metal whiskers at room temperature, which pose serious problems in the semiconducting industry [27–29]. The compressive stress is mostly accepted but insufficient condition for the growth of Sn, Cd, Zn, Al whiskers. It has been proposed that an oxidized surface must be thin enough to crack and to allow the extrusion of the compressed metal [27,28]. Other authors proposed recently an oxidation-based process, which assumes that oxygen diffuses and forms oxide at interfaces providing the driving force for whisker extrusion [29]. However, the whiskering phenomenon is not completely understood.

Based on the growth mechanism of compressive stress and subsequently relief of the stress, we propose a three-step model for the early stage formation of the MgH_2 nano-whiskers. At this stage, they are distinct and a growth model can then be suggested. During the first and second steps, the nucleation and growth of MgH_2 take place underneath the oxidized surface layer. Due to the hydrogen absorption an important expansion of the volume occurs (33% of volume expansion from Mg to MgH_2). During the third step, a compressive stress is induced and subsequently relieved by fracturing the oxidized surface and extrusion of the whiskers. For further heat-treatment cycles in hydrogen atmosphere, the growth mechanism of MgH_2 in polyhedral particles and intricate nets of whiskers is far from clear. Furthermore, the role of the Y hydrides in the formation of the whiskers is not yet elucidated. Improvements for understanding the formation of different morphologies of MgH_2 and the role of the Y hydrides in the growth of the whiskers are currently under investigation.

It is worth mentioning that previous hydrogenation studies on other rare-earth Mg materials did not show any whisker formation. Few studies have been reported regarding the microstructure of hydrogen decomposition phases of Mg-rich materials [16,17]. Theses reports have investigated the morphology of $CeMg_{12}$ [16] and $LaMg_{12}$ [17] after decomposition and showed a refinement of the grains together with an increased roughness of the surface.

4. Conclusions

We have found unique formation of a large number of single crystalline MgH_2 nano-whiskers by hydrogen induced disproportionation of bulk $Mg_{24}Y_5$. Occasionally, the whiskers have lengths and thicknesses in the micrometer range. The result opens new roads of designing Mg-based materials for different technological applications. The desorption of hydrogen and/or separation of these whiskers have not been investigated yet but might appear to be a promising approach for tailoring Mg assemblies with high active surface for hydrogen storage. Furthermore, it offers the unique possibility to study the physical properties of large MgH_2 single crystals. These features have never been investigated in bulk materials due to embrittlement by hydrogen absorption. Our results are a challenge for further experimental and theoretical work in order to understand the growth mechanism of MgH_2 whiskers and to study their physical properties.

Acknowledgments

This work was financially supported by the Swedish Energy Administration (STEM) and the Nordic Energy Research Project (NERP). The authors would like to thank to Ola Wilhelmsson for the help with the XPS measurements.

References

[1] P. Selvam, B. Viswanathan, C.S. Swamy, V. Srinivasan, Int. J. Hydrogen Energy 11 (3) (1986) 169.

[2] A.S. Pedersen. Hydrogen Metal System I, Solid State Phenomena 35, 1996, pp. 49–50.

[3] A. Zaluska, L. Zaluska, J.O. Ström-Olsen, Appl. Phys. A 72 (2001) 157.

[4] M. Pezat, B. Darriet, P. Hagenmuller, J. Less-Common Met. 74 (1980) 427.

[5] M.Y. Song, M. Pezat, B. Darriet, P. Hagenmuller, J. Less-Common Met. 103 (1984) 145.

[6] J.J. Reilly, R.H. Wiswall, Inorg. Chem. 7 (1968) 2254.

[7] C. Chacon, E. Johansson, C. Zlotea, Y. Andersson, B. Hjörvarsson, J. Appl. Phys. 97 (2005) 104903.

[8] P.J. Herley, W. Jones, B. Vigeholm, J. Appl. Phys. 58 (1985) 292.

[9] AMS International, Binary Alloys Phase Diagram, Second Edition plus updates, CD Version, 1996.

[10] J.F. Smith, D.M. Bailey, D.B. Novotny, J.E. Davison, Acta Metall. 13 (1965) 889.

[11] F. Bonhomme, K. Yvon, J. Alloys Compd. 232 (1996) 271.

[12] A. Fujimori, L. Schlapbach, J. Phys. C: Solid State Phys. 17 (1984) 341.

[13] P. Selvam, B. Viswanathan, C.S. Swamy, V. Srinivasan, J. Less Common Met. 163 (1990) 89.

[14] A.R. Miedema, Z. Metallkde. 69 (1978) 287.

[15] A.R. Miedema, Z. Metallkde. 69 (1978) 455.

[16] J.M. Boulet, N. Gerard, J. Less Common Met. 89 (1983) 151.

[17] M. Stoui, A. Grayevski, A. Resnik, D. Shaltiel, N. Kaplan, J. Less Common Met. 123 (1986) 9.

[18] The NBS tables of chemical thermodynamic properties, J. Phys. Chem. Ref. Data 11 (Suppl. 2) (1982).

[19] D. Sun, F. Gingl, Y. Nakamura, H. Enoki, M. Bououdina, E. Akiba, J. Alloys Compd. 333 (2002) 103.

[20] B. Bernhardt, K. Bohmhammel, Thermochim. Acta 382 (2002) 249.

[21] F.H. Ellinger, C.E. Holley Jr., B.B. McInteer, D. Pavone, R.M. Potter, E. Staritzky, W.H. Zachariasen, J. Am. Chem. Soc. 77 (1955) 2647.

[22] Y. Xia, P. Yang, Y. Sun, Y. Wu, B. Mayers, B. Gates, Y. Yin, F. Kim, H. Yan, Adv. Mater. 15 (2003) 353.

[23] Z.W. Pan, Z.R. Dai, Z.L. Wang, Science 291 (2001) 1947.

[24] J. Zhang, L. Zhang, X. Peng, X. Wang, Appl. Phys. A 73 (2001) 773.

[25] Z. Cui, G.W. Meng, W.D. Huang, G.Z. Wang, L.D. Zhang, Mat. Res. Bull. 35 (2000) 1653.

[26] K.A. Dick, K. Deppert, M.W. Larsson, T. Mårtensson, W. Seifert, L.R. Wallenberg, L. Samuelson, Nat. Mater. 3 (2004) 380.

[27] E. Iwamura, K. Takagi, T. Ohnishi, Thin Solid Films 349 (1999) 191.

[28] K. Zeng, K.N. Tu, Mater. Sci. Eng. R 38 (2002) 55.

[29] M.W. Barsoum, E.N. Hoffman, R.D. Doherty, S. Gupta, A. Zavaliangos, Phys. Rev. Lett. 93 (2004) 206104.